Pigment mass density and refractive index determination from optical measurements

1997 J. Phys.: Condens. Matter 9 1661

(http://iopscience.iop.org/0953-8984/9/7/027)

J. Phys.: Condens. Matter **9** (1997) 1661–1670. Printed in the UK PII: S0953-8984(97)74382-0

Pigment mass density and refractive index determination from optical measurements

William E Vargas and Gunnar A Niklasson†

Department of Materials Science, Uppsala University, Box 534, S-751 21 Uppsala, Sweden

Received 13 May 1996, in final form 12 November 1996

Abstract. The reflectance and transmittance of polymer films containing colloidal particles are characterized by specular and diffuse components which, for a given wavelength of the incident radiation, depend on particle size and composition, particle concentration, and film thickness. Pigment particles do not in general exhibit bulk densities or bulk optical constants. In this paper we introduce a method to determine the mass density and refractive index of non-absorbing or absorbing particles from experimental measurements. A four-flux radiative transfer model is used to describe the optical properties of dilute mixtures of silicon dioxide and titanium dioxide particles in a polymer matrix. The refractive index of the particles is varied from bulk values, in order to achieve good agreement with experimental reflectance and transmittance spectra. The obtained refractive indices can be related to the mass density of the particle material by the Clausius–Mossotti equation.

1. Introduction

Interaction of light with spherical particles has found a wide range of applications such as microwave and light reflection from rain in radar and meteorological uses [1, 2], infrared and visible reflection of paints which contain pigments [3, 4] such as titanium dioxide, zinc oxide, ferric oxide and molybdate orange. Other areas of actual interest are characterization of reflection and transmission by red blood cell suspensions, which could be used to gauge or to design medical instruments [5–7], light scattering by bacteria in water [8], improvement of solar radiation reflectance and thermal infrared properties in radiative cooling applications [9, 10], and production and characterization of composite silicon dioxide–titanium dioxide pigments which could be used as paper whiteners [11]. In the applications related to paper whiteners, radiative cooling, and white paints the suitable pigments should be characterized by a high reflectance of visible and near-infrared light. Consequently, these pigments should have high refractive indices which will lead to good scattering properties in this wavelength range. Among the most suitable materials is titanium dioxide which, in addition to its high refractive index, offers other advantages such as insolubility and stability through a great range of conditions and very low light absorption. Since its introduction as a commercial white pigment in 1941, the use of titanium dioxide has increased steadily.

The theoretical description of the optical properties of materials consisting of light scattering particles hosted in a dielectric matrix can be undertaken using transport theory. The term radiative transfer theory is also used to denote this approach in which it is assumed

† To whom correspondence should be sent.

0953-8984/97/071661+10$19.50

that there is no correlation between the fields scattered by the particles, and consequently the propagation of radiation is described in terms of specific intensities [12]. Diffraction and interference effects are included in the description of the scattering and absorption characteristics of single particles. For thick films under diffuse illumination, the two-flux radiative transfer model of Kubelka and Munk has been extensively used to predict the film optical properties [13, 14]. A four-flux radiative transfer model seems to be more appropriate when films are perpendicularly illuminated [15].

The purpose of this paper is twofold. First we present a theoretical framework for describing the optical properties of pigmented films. Lorenz–Mie computations for single particles are used in a four-flux radiative transfer model in order to obtain the specular and diffuse reflectances as well as the direct and diffuse transmittances. Effects of the substrate are also taken into account. The angular dependence of Lorenz–Mie scattering is taken into account only through so called forward scattering ratios. The use of single-particle scattering and absorption coefficients in the four-flux model means that dependent scattering is neglected. Secondly, we use the four-flux theory to describe experimental data on silicon dioxide (silica) and rutile titanium dioxide (titania) pigment particles in a polymer matrix. The samples are sufficiently dilute so that the independent scattering approximation holds. We find that theory and experiment can only be reconciled if the particle refractive index is lower than in the bulk. This refractive index can be related to the mass density in the particles. For both silica particles and titania ones, the obtained mass density corresponds very well to literature values. We propose the above method as a general tool for determining refractive indices and mass densities of pigment particles.

2. Extinction cross sections and forward scattering ratios of homogeneous particles

Given a homogeneous spherical particle of radius r and refractive index N_1, illuminated by electromagnetic radiation of free space wavelength λ_0, the size parameter and relative refractive index are defined as $x = 2\pi r N_2/\lambda_0$ and $m = N_1/N_2$ where N_2 is the refractive index of the surrounding medium. By expanding the incident, scattered, and internal electromagnetic fields in partial wave contributions, it is possible to obtain a description of the scattered radiation. We obtain from boundary conditions the so called scattering coefficients, a_n and b_n, where $n = 1, 2, \ldots$ specifies the order of the respective electric or magnetic partial wave. From the scattering coefficients one can evaluate the normalized scattering and extinction cross sections of the particle. These are given by [16, 17]

$$Q_{ext} = \frac{2}{x^2}\sum_{n=1}^{\infty}(2n+1)\,\mathrm{Re}(a_n + b_n) \tag{1}$$

$$Q_{sca} = \frac{2}{x^2}\sum_{n=1}^{\infty}(2n+1)[|a_n|^2 + |b_n|^2]. \tag{2}$$

The normalized absorption cross section is $Q_{abs} = Q_{ext} - Q_{sca}$. The explicit relations for the scattering coefficients were initially given for homogeneous particles [18], and later for composite ones [19]. Stable numerical algorithms have been developed to evaluate these scattering coefficients in terms of Ricatti–Bessel functions and their ratios [20].

For slightly absorbing or non-absorbing homogeneous dielectric particles, the dependence of the normalized extinction cross section on the size parameter shows two main features. These are a background oscillation which decays when the size parameter tends to infinity, and a ripple structure superimposed upon the main oscillation, after the position of the first peak [21, 22]. The amplitudes of the peaks in the main oscillation and in

the ripple structure increase as the real part of the particle refractive index increases, while their widths decrease. Both the main oscillation and the ripple structure tend to disappear as the imaginary part of the particle refractive index increases. The ripple structure has been explained in terms of resonances in partial surface waves which are specified by high-order scattering coefficients. These narrow peaks in the ripple structure have been observed experimentally in light scattering by growing water droplets [23], and by using optically levitated liquid drops [24]. The term morphological resonances is also used to denote these peaks in the ripple structure.

The resonances in the low partial waves have wide peaks which are superimposed in the largest peak of the main oscillation. This background oscillation has been interpreted as being produced by the interference between the forward scattered light and the incident beam, or the diffracted and transmitted light in the near-forward direction [25]. Consequently, this main oscillation is called the interference structure or large-scale oscillation. Films pigmented with strongly scattering particles, such as titanium dioxide in a polymer ($|m| \cong 2$), will display high diffuse reflectances under visible light incidence, while films containing weakly scattering particles will have a high direct transmittance.

Given a specific wavelength of the impinging radiation, the size of the hosted particles can be optimized in order to achieve high reflectance values. There is a correspondence between these high reflectances and the large scattering by the particles. Consequently, the optimization of the particle size can be established by maximizing its volumetric scattering cross section [26], C_{sca}/V, where V is the particle volume and $C_{sca} = \pi r^2 Q_{sca}$ is the particle scattering cross section. Another optimization criterion has been established in terms of the effective or reduced scattering cross section per unit volume, $(1-g)C_{sca}/V$, where g is the asymmetry factor, which can be evaluated from the scattering coefficients [27, 28]. By assuming perpendicular illumination, within the framework of a four-flux radiative transfer model, it has been established [29] that reflectances of films containing homogeneous pigments can be optimized in terms of pigment sizes which will lead to highest values of the backward hemispherical scattering cross section per unit volume, $(1-\sigma_c)C_{sca}/V$, where the forward scattering ratio under collimated incident radiation, σ_c, is given by [30]

$$\sigma_c = \frac{1}{2} - \frac{2}{\delta}\sum_{m=2}^{\infty}{}'' \sum_{n=1}^{\infty}{}'' p_{nm}\,\mathrm{Re}(a_m a_n^* + b_m b_n^*) - \frac{2}{\delta}\sum_{m=1}^{\infty}{}' \sum_{n=1}^{\infty}{}' q_{nm}\,\mathrm{Re}(a_m b_n^*). \tag{3}$$

Here $\delta = x^2 Q_{sca}$, and

$$p_{nm} = (-1)^{(m+n-1)/2}(2m+1)(2n+1)(m-1)!!n!!/(m-n)(m+n+1)m!!(n-1)!! \tag{4}$$

$$q_{nm} = (-1)^{(m+n)/2}(2m+1)(2n+1)m!!n!!/m(m+1)n(n+1)(m-1)!!(n-1)!! \tag{5}$$

$\sum'$ states a summation over odd integers, and $\sum''$ means another summation which is evaluated over even integers.

Given a spherical particle under isotropic incident radiation, the corresponding forward scattering ratio, σ_d, can be evaluated by expanding the particle phase function in terms of Legendre polynomials, and then by integrating it over the corresponding ranges of incident and scattering angles [31]. The result is

$$\sigma_d = \frac{1}{2a}\left[a + \sum_{n=1}^{\infty}{}' f_n g_n^2\right] \tag{6}$$

where $a = Q_{sca}/Q_{ext}$ is the particle albedo, and f_n are the coefficients involved in the expansion of the particle phase function [28]. They have been explicitly given by Chu and Churchill [32]. The coefficients g_n are given by

$$g_n = (-1)^{(n-1)/2}(n!!)^2/n(n+1)n! \qquad \text{when } n \text{ is odd, and zero otherwise.} \tag{7}$$

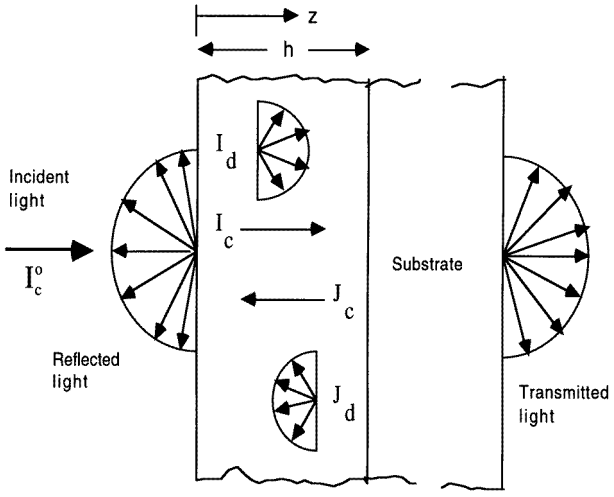

Figure 1. Electromagnetic radiation fluxes inside an inhomogeneous film of thickness h, which is normally illuminated.

The volumetric scattering and absorption cross sections, C_{sca}/V and C_{abs}/V, and the forward scattering ratios, σ_c and σ_d, play a major role in the four-flux radiative transfer model which we are going to summarize in the next section.

3. Reflectance and transmittance of inhomogeneous films

In order to study films containing homogeneous particles, a four-flux model [15] has been extended to take into account the substrate. An improvement of the model has been the evaluation, in an explicit way, of both the forward scattering ratio for collimated incident radiation, σ_c, and the corresponding parameter for diffuse incident illumination, σ_d, as indicated in the previous section. In this radiative transfer model, the radiation field inside the film consists of four contributions: two collimated beams (I_c and J_c) and two diffuse radiation fluxes (I_d and J_d), as indicated in figure 1. Perpendicular illumination is assumed, and the film is characterized by smooth interfaces with air and the substrate. The intensities of the collimated beams decay due to scattering and absorption by the particles. The intensity of the diffuse flux I_d is decreased by absorption, and scattering into the backward hemisphere (relative to the direction of the impinging radiation), and it is increased by scattering of the I_c, J_c, and J_d fluxes into the forward hemisphere. The corresponding analysis can be performed for the diffuse flux J_d. Consequently, the differential equations for the flux components are

$$\mathrm{d}I_c/\mathrm{d}z = -(\alpha+\beta)I_c \tag{8}$$

$$\mathrm{d}J_c/\mathrm{d}z = (\alpha+\beta)J_c \tag{9}$$

$$\mathrm{d}I_d/\mathrm{d}z = -\xi\beta I_d - \xi(1-\sigma_d)\alpha I_d + \xi(1-\sigma_d)\alpha J_d + \sigma_c\alpha I_c + (1-\sigma_c)\alpha J_c \tag{10}$$

$$\mathrm{d}J_d/\mathrm{d}z = \xi\beta J_d + \xi(1-\sigma_d)\alpha J_d - \xi(1-\sigma_d)\alpha I_d - \sigma_c\alpha J_c - (1-\sigma_c)\alpha I_c \tag{11}$$

where ξ is an average pathlength parameter: the average pathlength travelled by the diffuse beams as compared to the collimated ones. By considering isotropic diffuse illumination and neglecting the intensities of the collimated beams, the value $\xi = 2$ is consistent with

the Kubelka–Munk theory [33, 34]. By assuming a non-absorbing binder, and low particle concentration (neglecting dependent scattering effects) the film scattering and absorption coefficients per unit length are given by $\alpha = fC_{sca}/V$ and $\beta = fC_{abs}/V$, respectively. Here f is the particle volume fraction. The solutions for the collimated components can be easily obtained in terms of corresponding integration constants. Then, following Maheu *et al* [15], second-order differential equations for the diffuse components can be written in a concise notation, in terms of the following constants:

$$A = \xi\sqrt{\beta[\beta + 2\alpha(1-\sigma_d)]} \tag{12}$$

$$B = \alpha[\xi\beta\sigma_c + \xi\alpha(1-\sigma_d) + \zeta\sigma_c] \tag{13}$$

$$C = \alpha\{\xi[\alpha(1-\sigma_d) + \beta(1-\sigma_c)] - \zeta(1-\sigma_c)\} \tag{14}$$

$$D = \xi[\beta + \alpha(1-\sigma_d)] \tag{15}$$

$E = D - \xi\beta$, and $\zeta = \alpha + \beta$ as the extinction coefficient per unit length. By considering energy conservation across film interfaces, the solutions of the system of differential equations lead to explicit expressions for collimated and diffuse intensities [35], and reflectance and transmittance components [15]. For the reflectance, the specular and diffuse components are given by

$$R_{spec} = r_c + [(1-r_c)^2 F\,\mathrm{e}^{-2\zeta h}]/(1 - r_c F\,\mathrm{e}^{-2\zeta h}) \tag{16}$$

$$\begin{aligned} R_{diff} = {} & [(1-r_d)(1-r_c)\,\mathrm{e}^{-\zeta h}][C_0 + C_1\,\mathrm{e}^{\zeta h} + C_2\,\mathrm{e}^{-\zeta h}]/[(A^2-\zeta^2)(1-r_c F\,\mathrm{e}^{-2\zeta h})] \\ & \times\{[A(r_d G - 1)]C(Ah) + [E(G + r_d) - D(1 + r_d G)]S(Ah)\} \end{aligned} \tag{17}$$

where $C(Ah) = \cosh(Ah)$, $S(Ah) = \sinh(Ah)$, r_c and r_d are the reflection coefficients for collimated and diffuse radiation at the air–film and film–air interfaces, respectively, and

$$C_0 = A[(C + BF) - G(B + CF)] \tag{18}$$

$$C_1 = \{[A(BG - C)]\cosh(Ah) + [B(E - DG) + C(EG - D)]\sinh(Ah)\} \tag{19}$$

$$C_2 = F\{[A(CG - B)]\cosh(Ah) + [C(E - DG) + B(EG - D)]\sinh(Ah)\}. \tag{20}$$

Multiple boundary reflections in the substrate are taken into account by means of effective reflection coefficients for collimated and diffuse radiation at the film–substrate interface. These are given by

$$F = (r_c'[1 - 2r_c''\,\mathrm{e}^{-2\tau_s}] + r_c''\,\mathrm{e}^{-2\tau_s})/(1 - r_c' r_c''\,\mathrm{e}^{-2\tau_s}) \tag{21}$$

$$G = (r_d' + [1 - r_d' - r_d'']r_d'''\,\mathrm{e}^{-2\tau_s})/(1 - r_d'' r_d'''\,\mathrm{e}^{-2\tau_s}) \tag{22}$$

where r_c' (r_c'') is the reflection coefficient for collimated radiation at the film–substrate (substrate–air) interface, $r_d'(r_d''')$ is the reflection coefficient for diffuse radiation at the film–substrate (substrate–air) interface, and r_d'' is the reflection coefficient for diffuse radiation at the substrate–film interface. By means of the substrate optical thickness, τ_s, it is possible to incorporate the effect of substrate absorption. The transmittance components are given by

$$T_{spec} = \frac{(1-r_c')(1-r_c'')\,\mathrm{e}^{-\tau_s}}{1 - r_c' r_c''\,\mathrm{e}^{-2\tau_s}}\left[\frac{(1-r_c)\,\mathrm{e}^{-\zeta h}}{1 - r_c F\,\mathrm{e}^{-2\zeta h}}\right] \tag{23}$$

$$\begin{aligned} T_{diff} = {} & \{[(1-r_d')(1-r_d''')\,\mathrm{e}^{-\tau_s}(1-r_c)\,\mathrm{e}^{-\zeta h}][D_1\cosh(Ah) + D_2\sinh(Ah) + D_3\,\mathrm{e}^{\zeta h} \\ & + D_4\,\mathrm{e}^{-\zeta h}]\}[[1 - r_d'' r_d'''\,\mathrm{e}^{-2\tau_s}][(A^2-\zeta^2)(1 - r_c F\,\mathrm{e}^{-2\zeta h})]\{[A(r_d G - 1)]C(Ah) \\ & + [E(G + r_d) - D(1 + r_d G)]S(Ah)\}]^{-1} \end{aligned} \tag{24}$$

where

$$D_1 = A[(r_d C - B) + F(R_d B - C)] \tag{25}$$

$$D_2 = [(E - r_d D)(C + BF) - (D - r_d E)(B + CF)] \tag{26}$$

$$D_3 = A(B - r_d C) \tag{27}$$

$$D_4 = AF(C - r_d B). \tag{28}$$

By applying this four-flux radiative transfer model, using the scattering and absorption cross sections and forward scattering ratios from the Lorenz–Mie theory, total reflectances and transmittances ($R = R_{spec} + R_{diff}$ and $T = T_{spec} + T_{diff}$) were evaluated, and compared to measured ones.

4. Experimental results

We consider paints or films consisting of pigmented polymeric materials deposited on ordinary glass. Low-scattering films composed of silica particles, produced by the Stöber method [36], in a polymeric binder (Mowolith), as well as highly scattering rutile titania pigments (Flexonyl white R100 VP 2049, produced by Hoechst Inc.) in another polymeric matrix (Bindoplast, produced by Nordsjö-Nobel), will be used as examples of the method to obtain the particle mass density and refractive index. The thickness of the films was measured by using a Tencor Alpha-Step 200 surface profiling instrument, with values close to 70 μm for the samples considered here. Particles sizes close to 0.30 μm in diameter were obtained from scanning electron microscopy characterization. The displayed shape of the particles is spherical, with a fine surface roughness.

Reflectance and transmittance spectra were measured, for wavelengths between 0.30 and 2.5 μm (the solar range), using a Beckman 5240 spectrophotometer with an integrating sphere. Estimated errors were smaller than 1%. The optical constants of the polymer binders and the glass substrate were obtained from specular reflectance and direct transmittance measurements at near-normal incidence [37]. These materials are almost non-absorbing in the visible, and weakly absorbing in the near-ultraviolet and near-infrared wavelength ranges. The bulk optical constants for fused silica and rutile titania have been taken from the literature [38–41].

Experimental measurements are depicted in figure 2. The spectra of films containing silica particles are characterized by low reflectance values due to the weak scattering from these particles. The strong absorption in the near ultraviolet is mainly related to metallic impurities contained in the thick glass substrate [42]. The polymer binders cause a weak absorption band around 2.2 μm. Titanium dioxide pigmented films have high reflectance values in the visible wavelength range, where particle scattering reaches its highest values. For larger wavelengths (in the near infrared) of the incident radiation, the size parameter is lower, and consequently the scattering of the particles is decreased. The strong absorption in the near ultraviolet is due to interband transitions at about 3.02 eV [43].

5. Refractive index and mass density determination

By using the measured optical constants of the binders and substrate, and reported refractive indices for bulk silica and titania, predicted spectra for specific films, containing solid particles (i.e. particles characterized by a mass density corresponding to the bulk material), are depicted in figure 2. Calculated spectra were also obtained by varying the particle refractive index, and holding fixed the particle radius, pigment volume fraction, and film

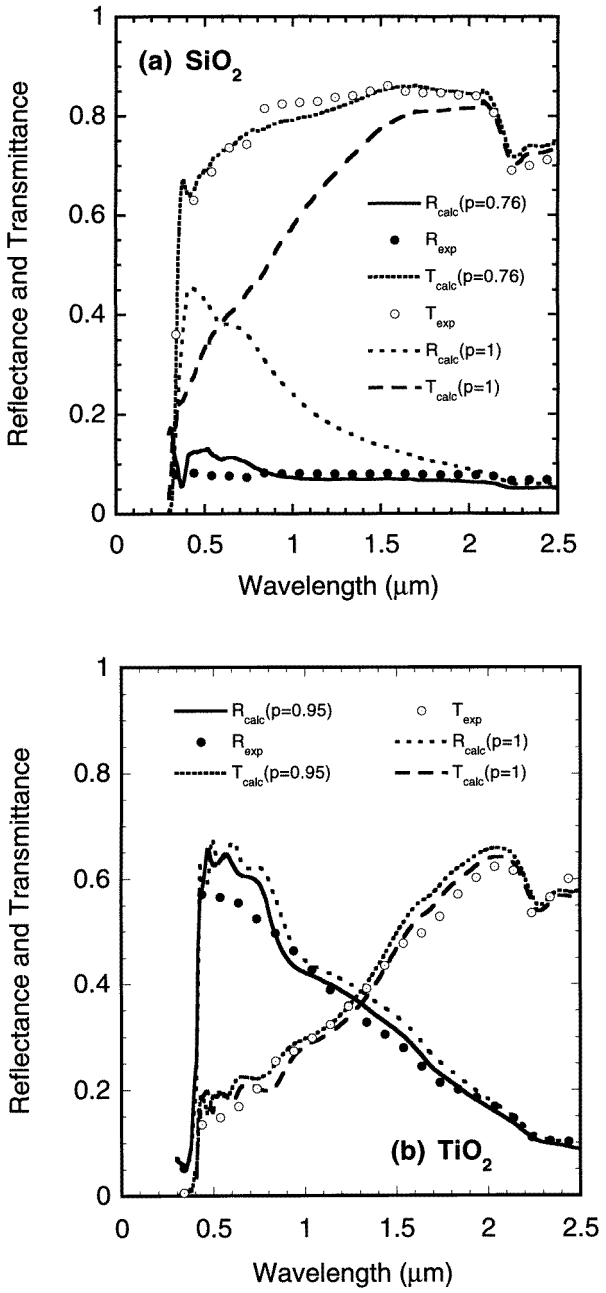

Figure 2. Experimental and calculated total reflectance (R) and total transmittance (T) spectra for films pigmented with (a) silicon dioxide (particle weight (volume) fraction and radius are 0.20 (0.125) and 0.15 μm respectively, with 70 μm as the film thickness) and (b) rutile titanium dioxide (particle weight (volume) fraction and radius are 0.05 (0.0125) and 0.15 μm respectively, with 67 μm as the film thickness). Points refer to experimental data and curves to calculated results (see the insets). The particle relative mass density is denoted by p.

thickness at values determined from independent measurements (see section 4), to obtain the best agreement with experimental data. The refractive index of a particle may differ

from that of the bulk material. Given the mass density (ρ_b) and refractive index of a bulk material ($m_b = n_b + \mathrm{i}k_b$), the presence of porosity in a specific sample leads to lower values of the real refractive index. This is a known effect in thin films for which the porosity is influenced by the film microstructure [44]. If a colloidal particle has some degree of randomly distributed porosity, its mass density and refractive index (ρ_p and $m_p = n_p + \mathrm{i}k_p$) can be established from the equation

$$\rho_p/\rho_b = [(m_b^2 + 2)/(m_b^2 - 1)][(m_p^2 - 1)/(m_p^2 + 2)] = p. \tag{29}$$

This result originates from the Clausius–Mossotti relation, where p is the particle relative mass density. By using this equation, with p as an unique fitting parameter, we establish the particle refractive index which leads to the best agreement between predicted and measured reflectances and transmittances. We vary p to minimize

$$F(p) = \sum_i^N \{|R_{exp}(\lambda_i) - R(\lambda_i, p)|^2 + |T_{exp}(\lambda_i) - T(\lambda_i, p)|^2\} \tag{30}$$

where N is the number of experimental measurements and $R(\lambda, p)$ and $T(\lambda, p)$ are evaluated from the four-flux model using the particle refractive index calculated from equation (29). In this way we get information about the particle optical constants and mass density.

Figure 2(a) depicts spectra of films containing silica particles with a measured particle weight (volume) fraction of 0.20 (0.125). The film thickness is 70 μm, and the particle diameter is 0.30 μm. The mass density of bulk fused silica [45] is 2.30 g cm^{-3}. The best fitting corresponded to a particle relative mass density of 0.76 which gives a particle mass density of 1.75 g cm^{-3}. This value is in very good agreement with a reported one, 1.80 g cm^{-3}, which characterizes colloidal silica particles produced by Stöber synthesis [36]. As also indicated in figure 2(a), predicted spectra are significantly different to measured ones, if we assume solid silica particles ($p = 1$).

Rutile titania is an optically anisotropic material, and for a polycrystalline sample one has to average the refractive index over the three principal directions. In our calculations for rutile we use this average bulk refractive index; this has been shown by Palmer *et al* [46] to be a good approximation when calculating scattering parameters. Figure 2(b) displays spectra of films containing rutile titania particles, with a measured particle weight (volume) fraction of 0.05 (0.0125). The film thickness is 67 μm, and the particle diameter is 0.30 μm. The mass density of bulk rutile titania [47] is 4.245 g cm^{-3}. In this case, the best fitting has been obtained for rutile titania pigments with very low porosity, characterized by a particle relative mass density of 0.95. Hence the mass density of these pigments is 4.03 g cm^{-3}. We also depict in figure 2(b) the calculated spectra when solid pigments are assumed. Even in this case of low-porosity pigments, the proposed criterion (equation (30)) allows us to discriminate between different relative mass densities: $F(p = 1.00) - F(p = 0.95) = 0.24$. Dumont *et al* have reported for spherical pure rutile hydrosols [48] a surface area of 9 m^2 g^{-1} with a very narrow size distribution (a mean diameter of 0.16 μm). From their data we can estimate the mass density of these titania hydrosols. It corresponds to a particle relative mass density of 0.98, which is also in very good agreement with the estimation for the pigments in our samples.

It has been established by Brewster and Tien that dependent scattering effects are influenced by the particle volume fraction, as well as the mean particle spacing in wavelength units [49], the so called particle clearance c/λ. For values of c/λ larger than 0.30, the independent scattering approximation is valid, otherwise the film optical properties will be influenced by dependent scattering effects. In our cases, for the titania pigmented film

c/λ is between 0.48 and 4.60, while the film containing silica particles is characterized by c/λ values between 0.13 and 1.30. Consequently, the spectra of the latter film are influenced by dependent scattering effects only in the near infrared, at wavelengths larger than 1.1 μm. In this wavelength range the scattering from the silica particles is small, and the film optical properties are mainly determined by the specular components of reflectance and transmittance. We can conclude that, in this case, the dependent scattering effects are weak enough to be neglected.

The predicted spectra for rutile display some valleys and peaks just after the absorption edge, which were not found in the measured spectra. We have observed that these peaks are directly related to corresponding peaks in the forward scattering ratios. As expected, they do not occur in the real spectra due to the fine surface roughness of the particles. Theoretically, the effect of particle surface roughness on the extinction cross section and forward scattering efficiencies has been studied by modelling the particle surface in terms of Chebyshev polynomials, and by applying T-matrix methods [50]. The peaks superimposed in the large-scale oscillation are suppressed or greatly damped when orientational averages are taken. As the wavelength of the incident radiation is increased, surface roughness effects tend to disappear, and a good agreement between measured and predicted spectra is observed. Size distribution effects, which we are not taking into account in the calculations, will also contribute to smooth the predicted spectra and suppress the ripple structure.

6. Conclusions

Within the independent scattering approximation, the optical properties of films containing particles with sizes comparable to visible wavelengths can be described by means of radiative transfer models. We evaluate scattering and absorption parameters of spherical particles from modal analysis. Subsequently, we use a four-flux model to obtain the reflectance and transmittance of films consisting of silica and titania particles in a polymer binder.

We are not aware of any systematic studies regarding comparisons between refractive indices of bulk materials and those of pigment particles. The results reported here show that, at least for chemically produced colloidal particles, the refractive indices can be significantly lower than values for the bulk material. The low particle refractive indices are modelled by the Clausius–Mossotti equation, assuming that the mass density of the particles is lower than bulk values. This procedure gives good agreement with experiments in the whole wavelength range that we consider. We propose that our simple optical technique can be used as a tool to determine refractive indices and mass densities of pigment particles. This method is also appropriate for use with films containing composite pigments, such as silica coated titania particles, which are being currently investigated as suitable pigments for paper and paints.

Acknowledgments

W E Vargas is grateful for the support that the Costa Rican National Scientific and Technological Research Council (CONICIT) and the University of Costa Rica have given to his work at Uppsala University. We also thank Professor J E Otterstedt and P Greenwood at Chalmers University of Technology (Goteborg, Sweden) for valuable discussions, and for preparing the samples whose optical properties have been considered in this paper. This work was supported by a grant from the Swedish Natural Science Research Council.

References

[1] Aden A L 1951 *J. Appl. Phys.* **22** 601
[2] Wang R T and Van de Hulst H C 1991 *Appl. Opt.* **30** 106
[3] Krewinghaus A B 1969 *Appl. Opt.* **8** 807
[4] Londergan M C and Spengeman W F 1970 *J. Paint. Tech.* **42** 260
[5] Steinke J M and Shepherd A P 1988 *Appl. Opt.* **27** 4027
[6] Graaff R, Aarnoudse J G, Zijp J R, Sloot P M A, de Mul F F M, Greve J and Koelink M H 1992 *Appl. Opt.* **31** 1370
[7] Streekstra G J, Hoekstra A G, Nijhof E J and Heethaar R M 1993 *Appl. Opt.* **32** 2266
[8] Waltham C, Boyle J, Ramey B and Smit J 1994 *Appl. Opt.* **33** 7536
[9] Niklasson G A and Eriksson T S 1988 *Proc. SPIE* **1016** 89
[10] Nilsson T M J, Niklasson G A and Granqvist C G 1992 *Solar Energy Mater. Solar Cells* **28** 175
[11] Hsu W P, Yu R and Matijevic E 1993 *J. Colloid Interface Sci.* **156** 56
[12] Ishimaru A 1976 *Wave Propagation and Scattering in Random Media* (New York: Academic)
[13] Klier K 1972 *J. Opt. Soc. Am.* **62** 882
[14] Phillips D G and Billmeyer F W 1978 *J. Coat. Technol.* **48** 30
[15] Maheu B, Letoulouzan J N and Gouesbet G 1984 *Appl. Opt.* **23** 3353
[16] Kerker M 1969 *The Scattering of Light and Other Electromagnetic Radiation* (New York: Academic)
[17] Bohren C F and Huffman D R 1983 *Absorption and Scattering of Light by Small Particles* (New York: Wiley)
[18] Mie G 1908 *Ann. Phys. Lpz.* **25** 377
[19] Aden A L and Kerker M 1951 *J. Appl. Phys.* **22** 1242
[20] Wiscombe W J 1980 *Appl. Opt.* **19** 1505
[21] Chylek P 1976 *J. Opt. Soc. Am.* **66** 285
[22] Chylek P and Zhan J 1989 *J. Opt. Soc. Am.* A **6** 1846
[23] Dobbins R A and Eklund T 1977 *Appl. Opt.* **16** 281
[24] Ashkin A and Dziedzic J M 1981 *Appl. Opt.* **20** 1803
[25] Lock J A and Yang L 1991 *J. Opt. Soc. Am.* A **8** 1132
[26] Faxvog F R 1975 *Appl. Opt.* **14** 269
[27] Blevin W R and Brown W J 1961 *J. Opt. Soc. Am.* **51** 975
[28] Gouesbet G, Grehan G and Maheu B 1983 *Appl. Opt.* **22** 2038
[29] Vargas W E and Niklasson G A 1995 *J. Colloid Interface Sci.* **169** 497
[30] Chylek P 1973 *J. Opt. Soc. Am.* **63** 1467
[31] Reichman J 1973 *Appl. Opt.* **12** 1811
[32] Chu C M and Churchill S W 1955 *J. Opt. Soc. Am.* **45** 958
[33] Kubelka P 1948 *J. Opt. Soc. Am.* **38** 448
[34] Maheu B and Gouesbet G 1986 *Appl. Opt.* **25** 1122
[35] Mudgett P S and Richards L W 1971 *Appl. Opt.* **10** 1485
[36] Coenen S and Kruif C G 1988 *J. Colloid Interface Sci.* **124** 104
[37] Vargas W E 1995 *MSc Thesis* Uppsala University
[38] Malitson I H 1965 *J. Opt. Soc. Am.* **55** 1205
[39] Ribarsky M W 1985 *Handbook of Optical Constants of Solids* ed E D Palik (New York: Academic) p 795
[40] Tang H, Prasad K, Sanjines R, Schmid P E and Lévy F 1994 *J. Appl. Phys.* **75** 2042
[41] Tang H, Berger H, Schmid P E and Lévy F 1994 *Solid State Commun.* **92** 267
[42] Smith H L and Cohen A J 1963 *Phys. Chem. Glasses* **4** 173
[43] Grant F A 1959 *Rev. Mod. Phys.* **31** 646
[44] Pulker H K 1979 *Appl. Opt.* **18** 1969
[45] Frederikse H P R 1963 *American Institute of Physics Handbook* ed D E Gray (New York: McGraw-Hill) ch 9, p 27
[46] Palmer B R, Stamatakis P, Bohren C F and Salzman G C 1989 *J. Coatings Technol.* **61** 41
[47] Tropf W J, Thomas M E and Harris T J 1995 *Handbook of Optics* ed M Bass (New York: McGraw-Hill) ch 23, p 42
[48] Dumont F, Warlus J and Watillon A 1990 *J. Colloid Interface Sci.* **138** 543
[49] Brewster M Q and Tien C L 1982 *J. Heat Transfer* **104** 573
[50] Wiscombe W and Mugnai A 1980 *Light Scattering by Irregularly Shaped Particles* ed D W Schuerman (New York: Plenum) p 141